Wall-Pressure Fluctuations of Modified Turbulent Boundary Layer with Riblets

Article *in* International Journal of Mechanical & Mechatronics Engineering · February 2016

CITATIONS
0

READS
24

1 author:

HAYDER A. ABDULBARI
Universiti Malaysia Pahang
96 PUBLICATIONS **110** CITATIONS

SEE PROFILE

Wall-Pressure Fluctuations of Modified Turbulent Boundary Layer with Riblets

Hayder A. Abdulbari[1,2*], Hassan D. Mahammed[1], Zulkefli B. Yaacob[1], Wafaa K. Mahmood[2]
[1] Faculty of Chemical and Natural Resources Engineering, Universiti Malaysia Pahang, Gambang 26300, Kuantan, Pahang, Malaysia,
[2] Center of Excellence for Advanced Research in Fluid Flow, Universiti Malaysia Pahang, Gambang 26300, Kuantan, Pahang, Malaysia

***Abstract*-- The experimental design incorporated to study the response of a turbulent pressure drop fluctuations to differently shaped longitudinal grooves, involved three conformations or structures being triangular, trapezoidal and spaced triangular grooves with height 800μm. The ratios of the groove height to groove space for triangular were: 1, 0.8, 0.6 and 0.4. Experiments were therefore performed at free stream velocity up to 0.44 *m/sec*, which were corresponding to Reynolds number (Re) 5.3×10^4. The development of the obtained turbulent layer downstream of the grooves was then compared with the results from the corresponding smooth-wall case. To conclude, the effect of the spaced triangular riblets on the turbulent characteristics seemed to be more pronounced than the effects of the triangular and trapezoidal riblets.**

***Index Term*-- Pipelines, Drag reduction, Skin friction, Riblets, Geometry**

1. INTRODUCTION

A reasonable amount of effort has been invested in studying the coherent structures in a turbulent boundary layer after the discovery of their prominent role in turbulent shear flows. Elaborate reviews and research can be referred with in Laufer [1], Willmarth [2], Antonia [3], Cantwell[4], Fiedler[5], Blackwelder[6] and Robinson [7],. All of these works provide a better insight and understanding of the working and structures pertaining to turbulent coherent structure.

Core changes towards turbulent structure and statistical analysis prove to be the determining factors of any drag reduction mechanism. As a result of which a varied amount of research has been invested towards the paradigm of manipulation of turbulent flow by applying drag reduction procedures.

The enhancing the flow of submerged surfaces using passive drag reduction techniques attracted enormous numbers of research activities in the past few decades due to its massive industrial and academic impact [8-15]. Among passive means, scientific researchers have much concentration on riblets and their drag reduction technique.

The Prime Concept being the use of a riblet surface, i.e. a surface with longitudinal micro-grooves, to obtain a skin-friction drag reduction by modifying the coherent structures of the turbulent boundary layer has its origin in these studies [15-23].

The most challenging task was determining the controlling drag reduction mechanism for all the researchers worked in this field due to the intensive chaotic nature of the turbulent flow media [24-27]. Generally, several tasks have been focused on during study the influence of riblets on turbulence structure and mean flow.

With optimal shaped and geometry, riblets are capable to reduce the drag reduction. Essentially they can reduce the drag force by approximately 10% when dimensionless rib spacing is 15–17 units [28].

The design of the grooves was meant to alter turbulence in the structures close to the near-wall region [29, 30]. Many investigations have been carried out, concerning the characteristics of modified turbulent boundary layer with riblets [18-23]. Turbulent flows exhibit effects of structured surfaces where they result in an increased surface area that cause a high shear force leading to an increment in pressure drop [31].

Several techniques have been used to measure the drag reduction, velocity and pressure measurements, flow visualization and direct numerical solutions to understand or to get a clue on what really happening over rib submerged surface in turbulent flow.

Wallace [32]reported the flow visualization on riblets for the very first time. This was also proved by the work that was published by Hooshmand et al. [33]. Both of them conducted their experiments on V-groove riblets. There was a minute variation in the structure of the boundary layer. Particles of smoke could be seen emanating from the V-grooves. The horizontal movement as well as the widespread of the reduced speed of the low streaks could be observed to have been dampened by the riblet grooves. Several riblets thereby adjoin with the structure of the wall just as the V-groove riblets.

Choi [34] discussed that in both the instantaneous wall shear stress measurements and the visualization of tapered rectangular riblets, the rectangular shaped riblets were used in to enable putting of a hot sensor in the groove valley. The momentum was noted to be very high on the top of these vortexes. In this, the smaller and the larger longitudinal riblets, all have a similar flow. In the findings of Choi, there was the fact that the tops on the wall shear stress were associated with the effect of the counter rotating vortices that were ran by the high momentum fluid[11].

Bacher and Smith, (1985) highlights the various effects of triangular V riblets on a turbulent wall. In their analysis, the viscous scale that was used was $h^+ = s^+$=15. There is

reduction in the lateral activity of the riblets. This is noted at the point where they have the highest effect on y^+<15. The riblets are very sluggish in their flow and do not show any spreading aspect laterally. It is also important to note that the drag reduction on the riblets cause is estimated to be 0.25%.

Seong[35] illustrate how the optimal factors can be developed through the application of Taguchi technique. The test was for the grooves that are on the top side of the circular cylinders. The study therefore highlighted the extrusive nature of particle image velocimetry an experimental tool that accommodates the collection of multi velocity vectors that are within the fields of flow.

From the study they conducted, there was a variation in the change of wake flow which was caused by the groove separation on the smooth cylinder. This separation is noted at 82 degrees. Tachie et al. [36] in his study, indicated that the coarseness of the ribs has a positive proportionality with the Reynolds stress by raising it as well as the triple velocity correlation. The effects of arranging the ribs adjacently on the turbulent fluid flow. In the study, they reiterate that the when the ribs are aligned in a perpendicular manner, to the side walls, the drag flow aspects are raised by a factor of almost 4.

Pressure is often chosen to characterize fluid dynamics of pipelines and channels. The advantage of using pressure is that it is easily measured, even under harsh, industrial conditions. A pressure measurement system, including pressure sensor and pressure tap, is robust, relatively cheap and virtually nonintrusive, thus avoiding distortion of the flow around the point of measurement.

Yet, the interpretation of pressure signals is far from straight forward. The main limitation in understanding the nature of the pressure signal lies in its intrinsically non-local nature. In that manner, the interpretation of pressure measurements is far more complicated than the measurements of the fundamental quantities. There have been a comprehensive review studies on pressure fluctuations in pipelines [37-42].

Investigation of wall pressure fluctuations in turbulent flow and their effect on a flat plate have been on table of interesting subjects for many years, but yet the amount of research still not covering the full point of view, especially when restructuring the surface of flat plate.

Lancey and Reidy[43] have conducted an experiment designed to work in a wind tunnel to investigate the effect of triangular rib surfaces on reduction of wall pressure fluctuations below a turbulent boundary layer. The triangular riblet has been manufactured by 3M Company with a height (h) and peak-to-peak spacing (s) of 0.152 mm for 30.5 m/s free-stream speed. A microphone with 0.762 mm diameter has been used to measure pressure frequency in each side of the tested plate. It was found that wall pressure over riblet have been reduced compare to smooth surface.

Keith [44] has measured the wall pressure fluctuations over triangular riblet in wind tunnel, under a turbulent boundary layer. The triangular riblet had height (h) and peak-to-peak spacing (s) of 0.0045. Two piezoelectric pressure transducers of diameter 2.032 mm. have been placed in the wall. The results presented shows not significantly changed in wall pressure by the presence of riblets.

Choi [45] carried out an experimental study in a wind tunnel over trapezoidal riblets with groove height (h) 1.5 mm and peak-to-peak spacing (s) of 2.5 mm. The wall pressure fluctuations were measured in a modified turbulent boundary layer with riblets and the results were compared with smooth surface. It was found that the riblets reduce the root mean square amplitude of pressure fluctuation by about 4% as also the turbulence near the wall. It seems that the riblets create pools of laterally constrained slow viscous flow in the valleys, and thereby modify the interaction of the wall flow with outer flow. The vertical gradients are thus smeared out, leading to a reduction in skin friction. An investigation was conducted by Dean & Bhushan [46] on the effect of riblets in internal rectangular duct flow. The flow cell has 1 m in overall length from inlet to outlet. It was fabricated in a way could change the duct's width to either 3cm or 4cm. Blade riblets with groove height (h) of 254 µm with three ratios of height to space equal to 0.3, 0.5, and 0.7 were fabricated. Their results showed increasing in pressure drop for all tasted rib surfaces comparing to smooth surface and no drag reduction recorded. Dean& Bhushan concluded that the reason of rib surface did not show overall benefit in reducing the drag, due to riblets dimensions as presented in their paper not beneficial in duct flow of that nature and dimensional characteristic.

In the present work; a new flow behavior detection technique is introduced through monitoring the pressure drop fluctuation over the structured surfaces (riblets). The new technique will utilize different riblets manufactured for the purpose of this work with different dimensions.

2. Experimental Set-up and Measuring Techniques

2.1 Experimental Apparatus

A schematic diagram of our experimental equipment is shown in figure (1). The experiment used. With 10 cm width of square channel through which fully turbulent water flowed, the range of Reynolds numbers was from 13000 to 53000 based on channel hydraulic diameter. Fluctuating pressure measurements in the channel wall were taken with great care to eliminate all vibration in the experimental equipment. Tap water was used and repeatedly changed after each series of tests. A supply tank is rectangular in shape at a height of 520 mm, width of 300 mm and 500 mm in length. Centrifugal pump connected to the tank from the bottom and it has the capability to drive the primary fluid at a rate of $36 m^3/hr$.

Water is pumped from the centrifugal pump, from the supply tank, into the PVC pipes (2 inches in size), then through the test section, and into the supply tank again. A bypass was provided in order to regulate the amount of water being pumped to the channel then to the supply tank again. The square channel of the experimental rig has been designed and fabricated in such a manner that there are four transparent polycarbonate plates with dimensions $(2\times0.12\times0.01)m$, which have been used to fabricate the channel.

Acrylic welding was used in fabrication of all the sections of the channel, Acrylic softens the plate surfaces, allowing them to merge and become one part, rendering much more strength to the channel and preventing leakages. The channel easily removed from the system by two side part sections fabricated on trapezoidal shape. The slides have two open ends, square and circle ends which used to connect the PVC pipe to the channel.

Care was exercised to ensure alignment each time this was carried out. Two pressure tabs are placed at the bottom surface of the channel used for measuring the pressure drop. These tabs comprised the test sections, where $0.16m$ placed at the end for the channel get full turbulence flow. The pressure drop is taken for this section over the smooth plate and rib surfaces. A flow meter that is located in the flow duct to records the amount of water flowing through the rig before it proceeds on to the pressure transmitter. Pressure tap points of 12.7 mm in diameter were provided at the bottom of the channel. Each of these pressure tap holes span more than one groove, depending on the width of the grooves. The pressure drop was measured by the differential pressure transducer.

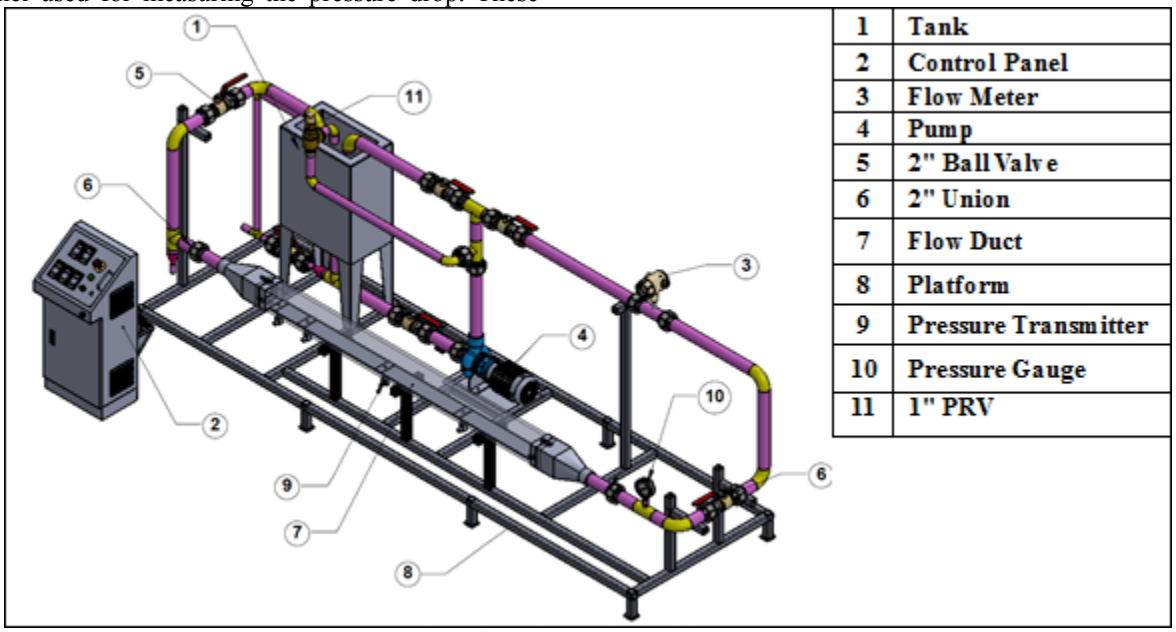

1	Tank
2	Control Panel
3	Flow Meter
4	Pump
5	2" Ball Valve
6	2" Union
7	Flow Duct
8	Platform
9	Pressure Transmitter
10	Pressure Gauge
11	1" PRV

Fig. 1.Shows the experimental rig.

2.2 Riblets Dimension and Fabrication

The riblets models were fabricated longitudinal to the direction of the stream wise with the characteristic dimensions listed in Figure 2.

The process of manufacturing involved first milling 12 pieces of 160 mm long, 80 mmwide and 8mmthick, flat Aluminium sheets with CNC machine. After machining, the sheets were cut to size of the test section that papered in the square test channels. Then the rib surfaces were fabricated with wire electrical discharge machining (WEDM). The size of the grooves and the length of the test sections were therefore dictated by the size of the cutting wire (150 µm). Figure 2, illustrates grooves that are defined by peak height (h), peak-to-peak spacing (s), groove tips (τ)and groove base (ω)with selected dimensions.

Three different groove shapes have been fabricated and tested: triangular, trapezoidal, and spaced triangular riblets were investigated. Each groove shape has the same groove height (h) equalling 800µm but have different groove space. The triangular and trapezoidal both have same groove dimensions (height and space) except the trapezoidal tip which have been given relatively to peak-to-peak spacing($\tau = 0.2S$), in order t o investigate the effect of tips edge on the pressure fluctuation s and turbulent flow.

The spaced triangular riblets have been fabricated in a way where the base of spaced triangular groove(ω) is equal to peak-to-peak spacing(s)of triangular and trapezoidal riblets.

More over the peak-to-peak spacing(s) was twice the spacing in triangular and trapezoidal riblets

The main purpose of the present study is to investigate the response of turbulent flow to longitudinal grooves of various shapes and compare the effect of the turbulence structure over smoothed and grooved surfaces with pressure drop measurements.

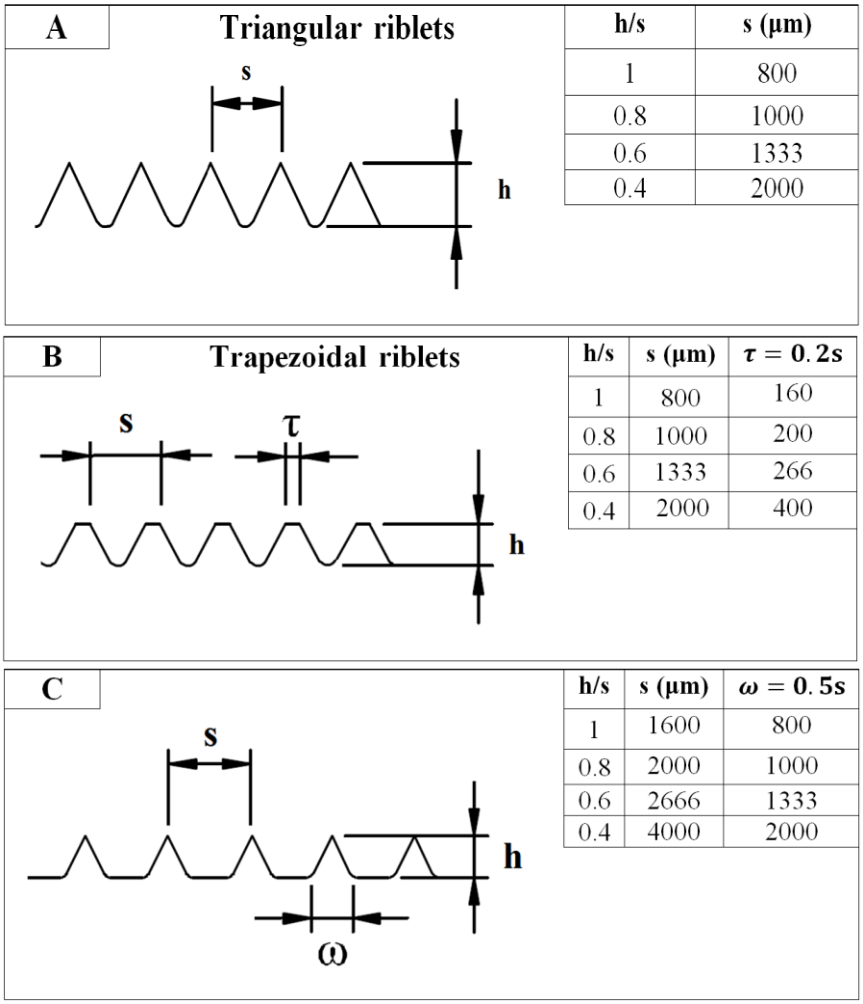

h/s	s (μm)
1	800
0.8	1000
0.6	1333
0.4	2000

h/s	s (μm)	$\tau = 0.2s$
1	800	160
0.8	1000	200
0.6	1333	266
0.4	2000	400

h/s	s (μm)	$\omega = 0.5s$
1	1600	800
0.8	2000	1000
0.6	2666	1333
0.4	4000	2000

Fig. 2. Dimensions of fabricated grooves have same heights (h=800μ)
(A)Triangular riblets (B) Trapezoidal riblets (C) Spaced triangular riblets

2.3 Measurements

The skin friction coefficients (C*f*) and Reynolds numbers (Re) were calculated from the wall shear stress and flow rate measurements by using the following equations:

$$Cf = \frac{2\tau_w}{\rho\, u^2} \text{ and } Re = \frac{u\, D_h}{\upsilon} \quad (1)$$

Where (u) is mean velocity (m/sec),
(υ) is the kinematic viscosity of water (m^2/sec),
(ρ) is the density of water (Kg/m^3) and (τ_w) is the wall shear stress in a fully developed pipe flow, as defined by Perry et al.[48].

This equation relates the wall shear stress to the pressure drop during the turbulent flow inside the pipelines.

$$\tau_w = \frac{\Delta p\, D_h}{4L} \quad (2)$$

The percentage drag reduction (DR %) is defined as:

$$DR\% = \left(\frac{\Delta P_{Smooth} - \Delta P_{riblet}}{\Delta P_{Smooth}}\right) \times 100 \quad (3)$$

The diameter used in the calculation of the Reynolds number and friction coefficient is defined as hydraulic diameter $D_h = 4\frac{A}{p}$, where (A) is the area section of the duct and (p) is the wetted perimeter of the duct.

3. Experiment Results and Discussion

3.1 Pressure fluctuation signals over smooth and rib surfaces

Ideally, the effect of longitudinal grooved surfaces on wall-pressure fluctuations can be determined by comparing measurements made on smooth and rib flat plate at exactly the same Reynolds number and surface roughness.
The time series of the pressure: is known to have very distinct specific aspect. The simplest analysis in time domain is to plot a sequence of data points of the measured signal which will give a qualitative description of the time scale and of the complexity of the flow. As far as the signal of the pressure is concerned, which is characterized by random fluctuations that revolve around the given pressure mean value. Turbulent flow is characterized by fluctuations in pressure, acceleration and shear stress, all associated with position and time.

As a result of these fluctuations, the velocity and pressure terms in the momentum and energy equations, shows varied difference. In order to investigate the effects of groove shapes and size on pressure fluctuations three shapes have been chosen to fabricate with same groove height and have different groove space.

The triangular and trapezoidal riblets have groove space of 800, 1000, 1333 and 2000μm to investigate the effect of the edge sharpness on the drag force. But for spaced triangular the groove dimensions was double size of triangular to investigate the effect of the groove space on drag force. Figures 3 to 5 show the pressure drop fluctuations over the smooth and riblet plates at Reynolds number 5.3×10^4.

To gain deeper understanding of the controlling mechanism of the drag reduction and radical behavior of the grooved surfaces, the pressure drop readings for each surface and the flow rate are simultaneously recorded over 60's. There are at least two groups of fluctuations that make up the wall pressure. This is according to the suggestion provided by the collective body of results [49-52]. The first group of pressure fluctuation signals is made up of large-scale disturbances that are of low-frequency. Such disturbances come from the surrounding portions of the boundary layer and goes up to within the unsteady potential flow. The large-scale disturbances remain consistently on course with the character of the interface of the potential flow which is outside the boundary layer. On the other hand, the second group of pressure fluctuation is made up of small-scale disturbances that are of high-frequency and are considered to have a relation with the burst-sweep cycle of events. Such disturbances are also noted to follow the wall pressure fluctuations of large-amplitude.

Figure 3 shows the pressure readings at Reynolds number = 5.3×10^4 for triangular grooves. The resultant results shows that the pressure drop readings that were performed on the surface are more stable, and that also its turbulence frequency is low as compared to other surfaces. Moreover, most of the pressure drop point lies below the smooth surface pressure drop line with higher irregular or less smooth readings. The structured surfaces tends to portray pressure readings that have higher amplitude, as well as the readings where the smooth surface is tested but their average readings when taken into consideration tends to be a little lower. Statistically, the structured surfaces portrays on an average basis pressure drops that are a little bit lower even though the figures show certain points with higher pressure drop values. This can then be explained by the fact that the reason for the structure surfaces displaying; the low-pressure drop readings is that on the initial phase the pressure drops had to stabilize for a certain period of time before proceeding to return to the same smooth surface readings. The same pattern is reaped for over many period of time explaining the low-pressure drops that are shown on an average basis.

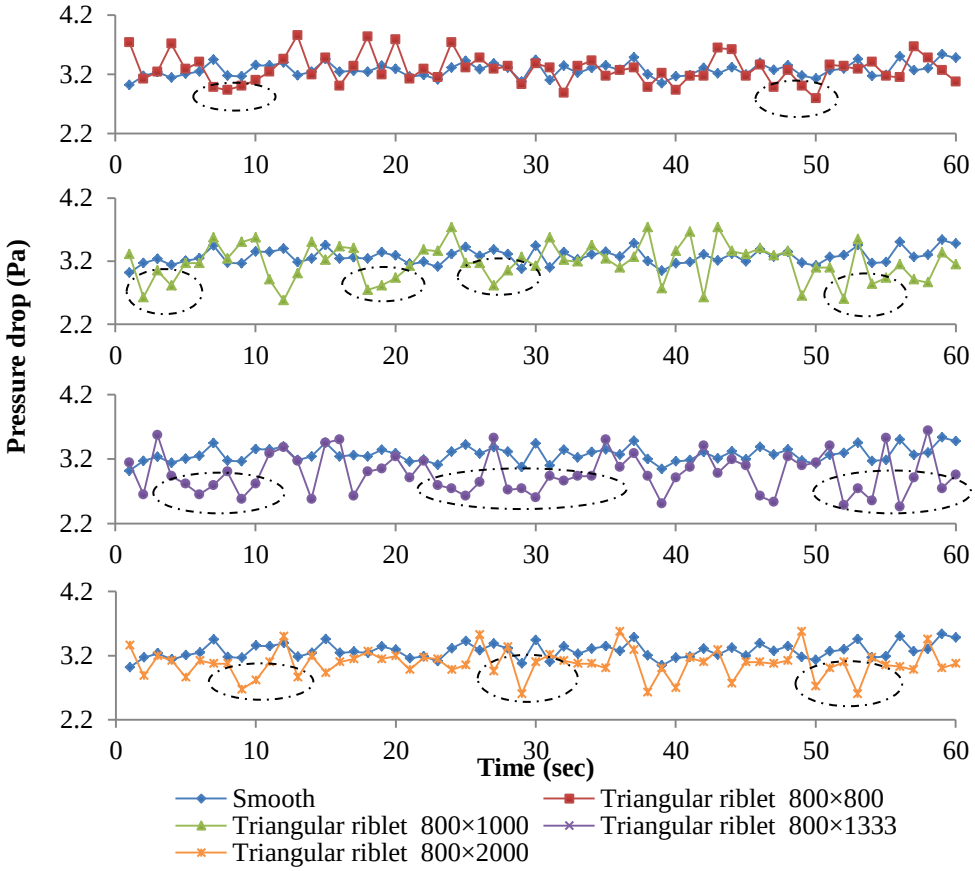

Fig. 3. Pressure fluctuation time series at Reynolds number 5.3×10^4 for smooth and triangular riblet

The pressure drop in Figure 3 is clearly reduced when the groove space is 1000, 1333, and 2000 µm, with clearly distinguished low stable pressure drop areas. But interestingly to note that those stabilized areas of pressure drop appeared at almost same period of time in those riblets and give an indication that riblets enhanced the turbulent fluctuation.

For groove space 800 µm, the pressure fluctuations tends to shift to the opposite direction or against the direction that the pressure drop readings start to have higher or same amplitude as smooth plate and less stable low reading zones. This is the same principle that explains why a triangular riblet plate with dimensions of 800 µm × 1333 µm tends to exhibit the best performance among all the selected triangular riblet dimensions, as shown in Figure 3. In particular, the frequency and pressure drop of this plate become lower at the same period of time and at the same Reynolds number, relative to those of the smooth plate.

Figure 4 shows the pressure drop reading of trapezoidal riblets with height equal to 800 µm and space 800, 1000, 1333 and 2000µm. The results shows that low-pressure drop zones are always represented as highly non-linear with an increase in groove space.

The pressure drop is low when the groove space value was 800, 1333, 2000 µm. But no significant change is observed on the structured surface of size 1000 µm. The trapezoidal riblet plate with dimensions of 800 µm × 800 µm in this category demonstrates the best performance among the selected trapezoidal riblet dimensions.

Applying the trapezoidal riblet to the channel has a way of causing fluctuation in the pressure drop reading as compared the smooth plate, It is also worthy to note that the frequency and pressure drop exhibited become lower at the same period of time and at the same Reynolds number 5.3×10^4.In general, pressure signals over the riblets of the triangular and trapezoidal have the same signal pattern behavior and slightly different magnitude and this could be seen when in figures 3 and 4 especially with groove dimension 800 µm × 1333µm which means the tip geometry do not affect significantly the pressure fluctuations.

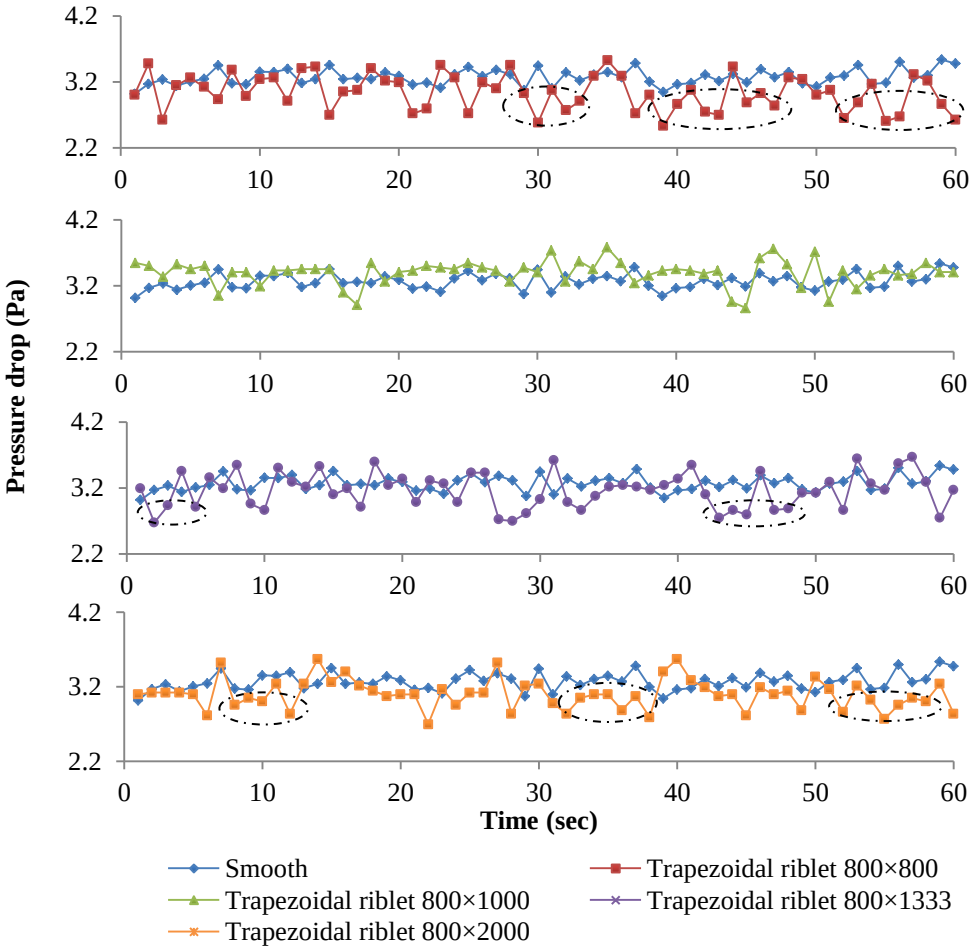

Fig. 4. Pressure fluctuation time series at Reynolds number 5.3×10^4 for smooth and Trapezoidal riblet

Figure 5 shows the pressure fluctuation time series at Reynolds number 5.3×10^4 for smooth and spaced triangular riblets. The results show a real and effective riblets performance with very wide and more stable low pressure drop zones that can cover almost the whole testing time period. The spaced triangular riblet plate with dimensions of

800 µm × 4000 µm shows the best performance in reducing the drag reduction among the selected spaced triangular riblets dimensions but the pressure drop fluctuation signals is high compare to the smooth surface.

Furthermore, spaced triangular riblet plate with dimension 800 µm × 2666µm shows almost the same sequence period of stabilized areas of pressure drop that appeared in triangular and trapezoidal riblet plate with dimensions 800 µm × 1333µm. Interestingly to note that pick-to–pick spacing of this plate is twice the spacing of triangular and trapezoidal riblet plate.

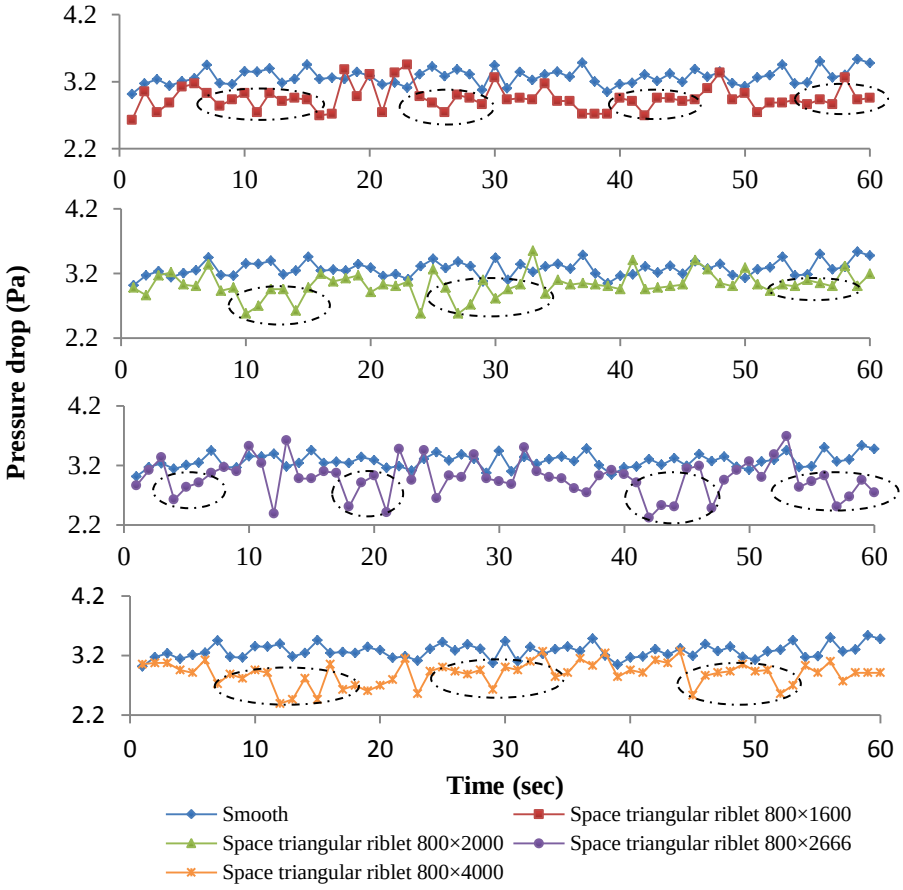

Fig. 5. Pressure fluctuation time series at Reynolds number 5.3×10^4 for smooth and spaced triangular riblet

Figures 6 to 8 show a comparison in pressure drop fluctuations over the smooth and riblet plates at difference Reynolds number. The large peaks that are observed in some points comes' as a result of the strong depressions experienced in the mode. Each and every strong peak that is experienced in the pressure signal is due to a filament with an extremity attached to the wall passing to the transducer. The consequence of this arrangement is that at the end, all the filaments passing through the transducer have a way of causing a deep peak in the pressure signal. The shape of the signal corresponding to a filament passing directly on the probe reflects its exact present state. The only time that pressure drop experienced in the time series can be deep and narrow is only when the filament that passes through the transducer has recently been formed and assumes a straight shape in its formation. If the filament is undergoing a vortex breakdown, then the overall depression is still deep but is now broader, and the signal exhibits multiple secondary negative peaks.

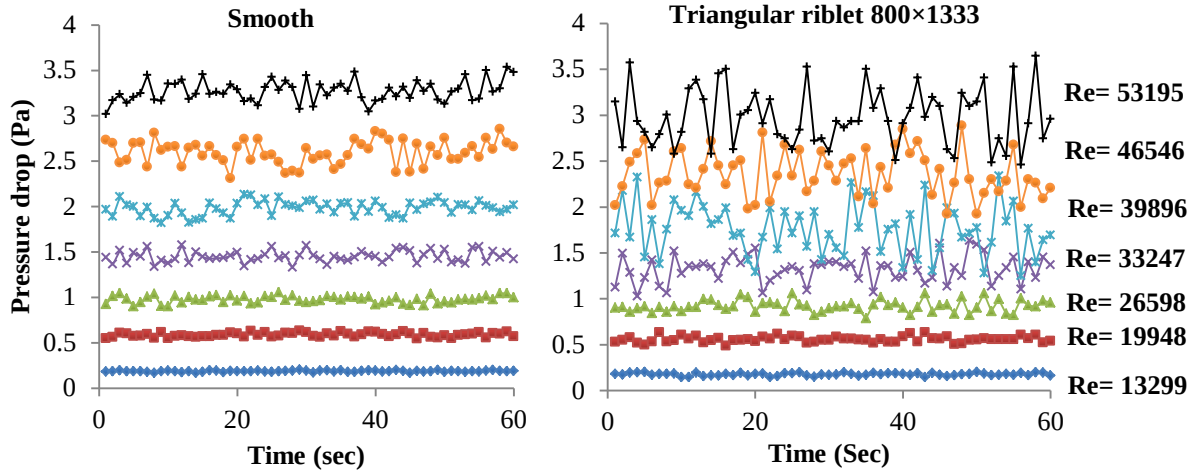

Fig. 6. The profiles of pressure fluctuation time series under different Reynolds number for smooth and triangular riblet 800×1333μm

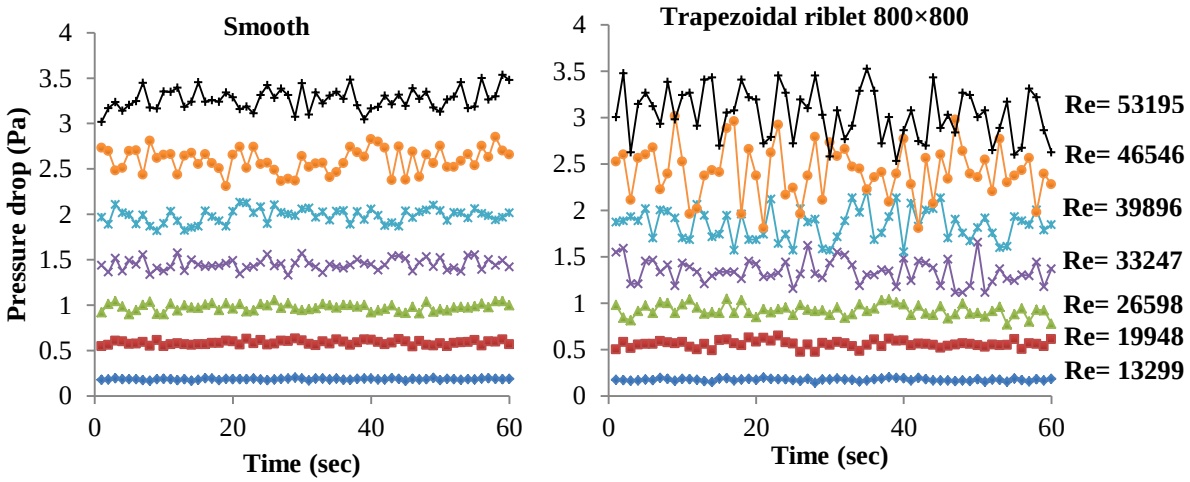

Fig. 7. The profiles of pressure fluctuation time series under different Reynolds number for smooth and trapezoidal riblet 800×800μm

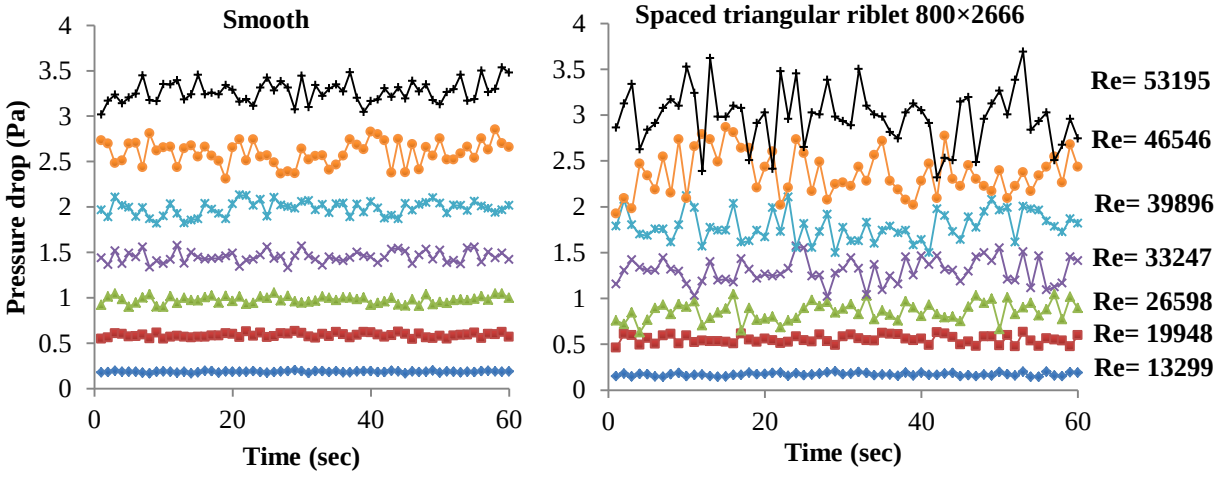

Fig. 8. The profiles of pressure fluctuation time series under different Reynolds number for smooth and spaced triangular riblet 800×2666μm

3.4. Effects of Pressure Drop over Smooth and Rib Surfaces

In this study, the Reynolds number from 13000 to 53000 was studied. Figures 9 to 11 compare the pressure drop measured across the smooth plate and all the riblet surfaces tested in the channel and plotted against the Reynolds number, which is calculated using Equation (1).

This start falls in the agreed margin of a Reynolds number that ranges from $1.3 \times 10^4$to 1.9×10^4. Typically, any form of any increase in the rate of pressure drop can be arrived upon as the Reynolds number increases. Afterward, the resultant divergence zone is the Reynolds number would be ranging from$1.9 \times 10^4$to 5.3×10^4, which is characterized

by the pressure drop of the tested plates continue rising on a continuous basis.

By contrast also is the fact that the results of the given spaced triangular riblet dimension is used to demonstrate the beneficial trend that is always relative to the smooth surface for the entire range of the tested Reynolds number. A common trend here is that a decreasing rate in the pressure drop is always eminent.

Figure 9 is used to show the effect of the selected triangular groove on improving the flow of water inside the channel. It is then noted as shown from the figure, that whenever the Reynolds number is increased together with the different triangular riblet sizes considered in the experimental work has the consequent of increasing the rate of the pressure drop for the tested plates. Two well-defined zones then come into the picture and can easily be spotted out. This are the convergence zone where the pressure drop of the triangular grooved surfaces and that of the smooth surface are close to a Reynolds number ranging from $1.3 \times 10^4$to 2.6×10^4 are usefully used to depict a steady increase in the rate of pressure drop as the Reynolds number increases. The other notable zone is the pressure drops of the tested plates that has a way of rising on a continuous basis and start to diverge to the Reynolds number ranging from 2.6×10^4 to 5.3×10^4. On the hand, its worthy to note that the results of the triangular riblet dimensions are used to show a beneficial trend compared with the smooth surface for the entire range of the tested Reynolds number.

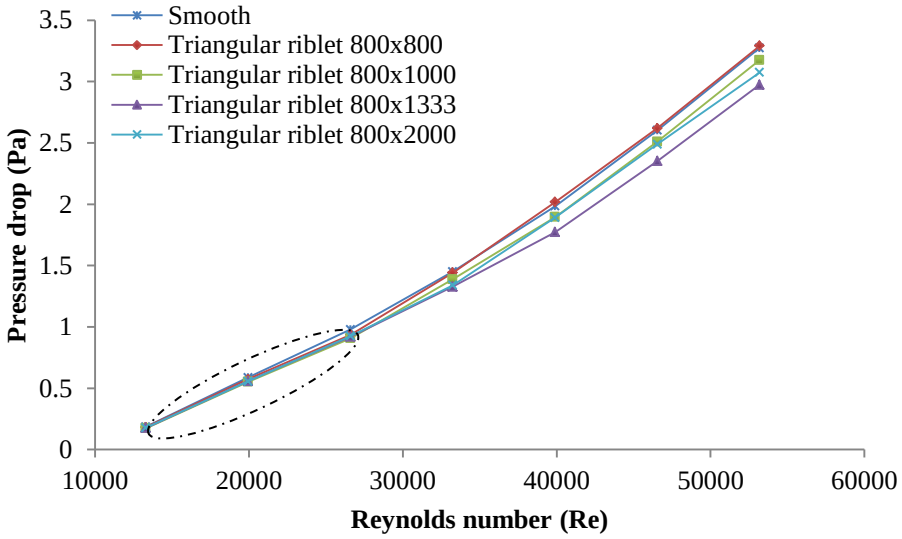

Fig. 9. Pressure drop comparison over smooth and triangular groove.

Figure 10 shows the effect of the selected trapezoidal riblet on improving the flow of water inside the channel. The general behavior is the same as that described in Figure 9. However, the convergence zone starts with a Reynolds number ranging from $1.3 \times 10^4$to 3.3×10^4, where a steady increase in the rate of pressure drop is generally observed as the Reynolds number increases. The pressure drop of the tested plates in the divergence zone has a way of rising on a continuous basis to a point that it starts to diverge from the Reynolds number ranging from $3.3 \times 10^4$to 5.3×10^4. One of the selected dimensions of the trapezoidal riblet, with a height of 800 μm and spacing dimension of 1000 μm, shows no beneficial trend relative to the smooth surface for the entire range of the tested Reynolds number. This is explained by the fact that an increasing rate in the pressure drop is significantly noted relative to the range of the tested Reynolds number over the smooth plate. To sum up it all in a more comprehensive manner, all the behavior and relation between the pressure drop and Reynolds number tends to be the same as the ones that Figures 9 and 10 depicts.

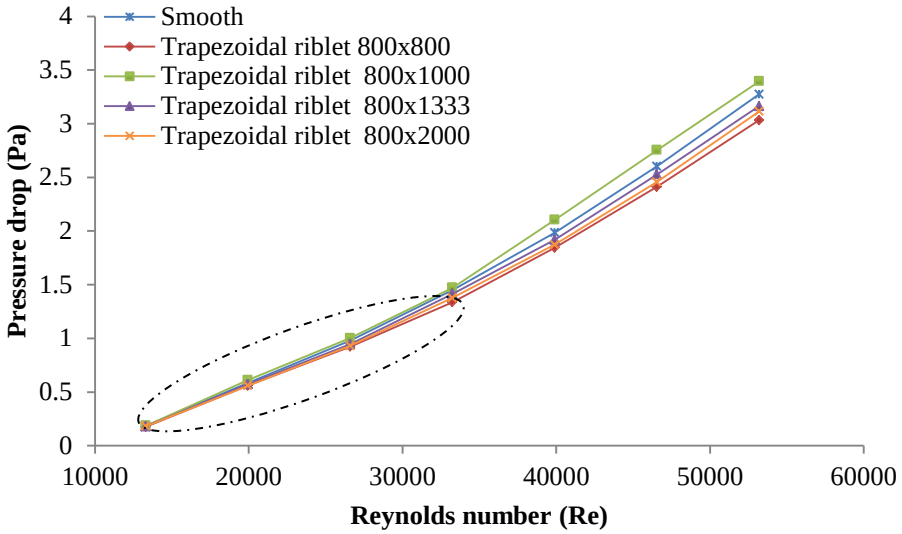

Fig. 10. Pressure drop comparison over smooth and trapezoidal riblet.

This trend is also evidently true in Figure 11, which shows the effect of the selected spaced triangular riblet on improving the water flow inside the tested channel. The results of the selected spaced triangular riblet dimensions reveal a decreasing rate in the pressure drop compared with the smooth surface for the entire range of the tested Reynolds number.

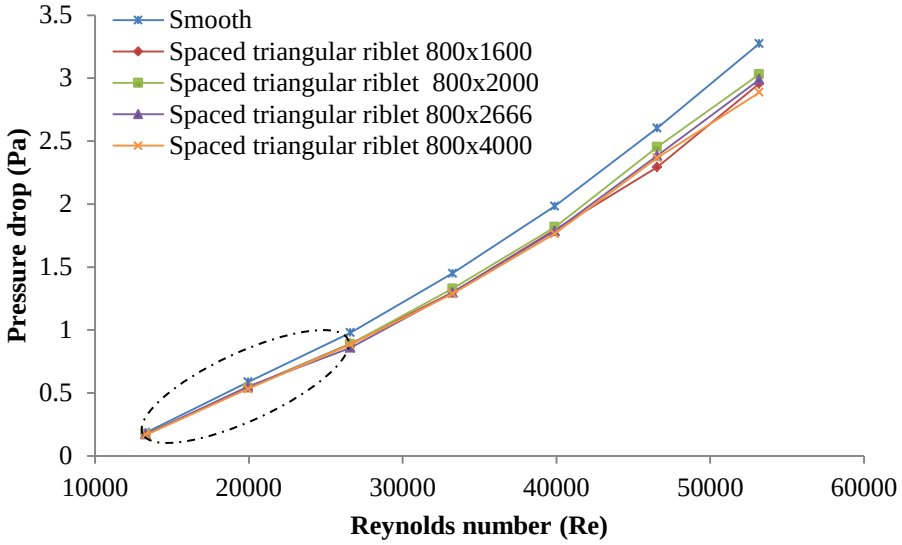

Fig. 11. Pressure drop comparison over smooth and spaced triangular riblet.

3.5. Effect of Reynolds Number over Smooth and Rib Surfaces.

The typical results that illustrate the effect of the Reynolds number on the percentage of drag reduction with different rib spaces and different riblet surface shapes, as tested in the channel, are shown in Figures 12 to 14. A comparison of the percentage of drag reduction measured across the selected triangular riblet surfaces tested in channel are shown in Figure 12. Generally observed in all the investigated triangular riblets, the drag reduction percentages initially increase when the flow rate represented by the Reynolds number is increased until some point then drop down and decreasing the percentage of drag reduction. The increasing behavior is due to the decrease in the turbulence degree and interaction degree between the grooved surface and the turbulent structures formed inside the channel. Accordingly, the groove riblets are able to interfere with the turbulent median and to suppress eddies formed inside the channel, which in turn improves the flow. A further increase in the Reynolds number allows the turbulence degree to overcome the effect of the drag reduction ability of riblets, and the curves start to show descending values of the reduction percentage. In this case, the current riblets at that flow rate are

no longer capable of overcoming the chaotic movement of the flow in the channel.

At a Reynolds number of 2.6×10^4, the drag reduction percentage for the triangular riblet with spacing dimensions of 800, 1000, 1333 and 2000 μm is 4%–7%, whereas the drag reduction percentage for triangular riblet with a spacing dimension of 750 μm is 10.8%.

Figure 13 shows a same behavior from that described in Figure 12. This figure shows the effect of the trapezoidal riblet on improving the turbulent flow of the water inside the channel. The relation between the percentage of drag reduction and Reynolds number is smoother than that shown in Figure 12. In general, the curves of the trapezoidal riblet with spacing dimensions of 800, 1333, and 2000 μm continue to increase when the Reynolds number increases. Meanwhile, the curve of the trapezoidal riblet with spacing dimensions of 800 μm × 1000 μm shows no positive percentage of drag reduction. However, the behavior and relation between the percentage of drag reduction and Reynolds number tend to be the same as those described in Figure 12.

The behavior and relation between the percentage of drag reduction and Reynolds number in Figure 14 are the same as those shown in Figure 12. In general, the spaced triangular riblets continue to increase when the Reynolds number increases. Meanwhile, the curve of the spaced triangular riblet with spacing dimensions of $800\ \mu m \times 2666\ \mu m$ initially reaches its maximum at a Reynolds number of 2.6×10^4 with a value of 12.3 and then starts to decline reaching a value of 8.4 at a Reynolds number of 4.6×10^4.

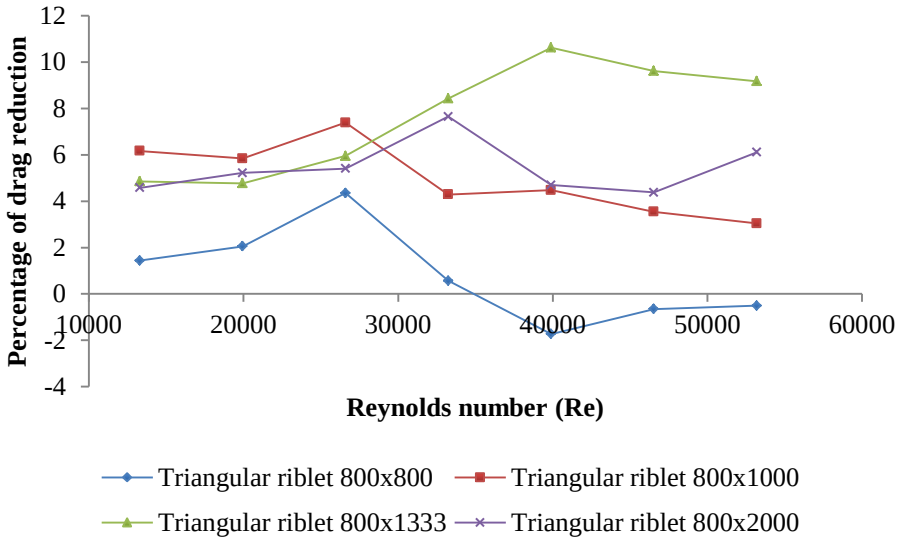

Fig. 12. Effect of Reynolds number on the percentage of drag reduction for triangular riblets.

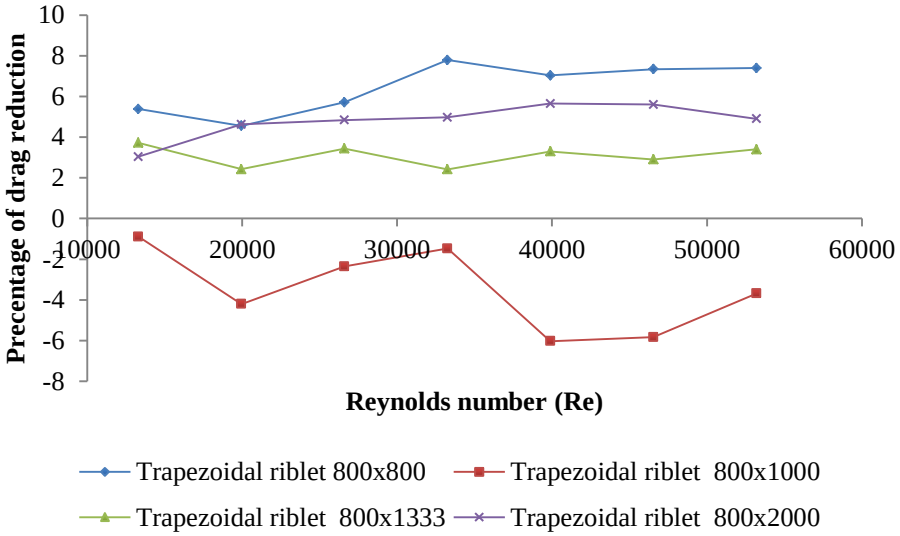

Fig. 13. Effect of Reynolds number on the percentage of drag reduction for trapezoidal riblet.

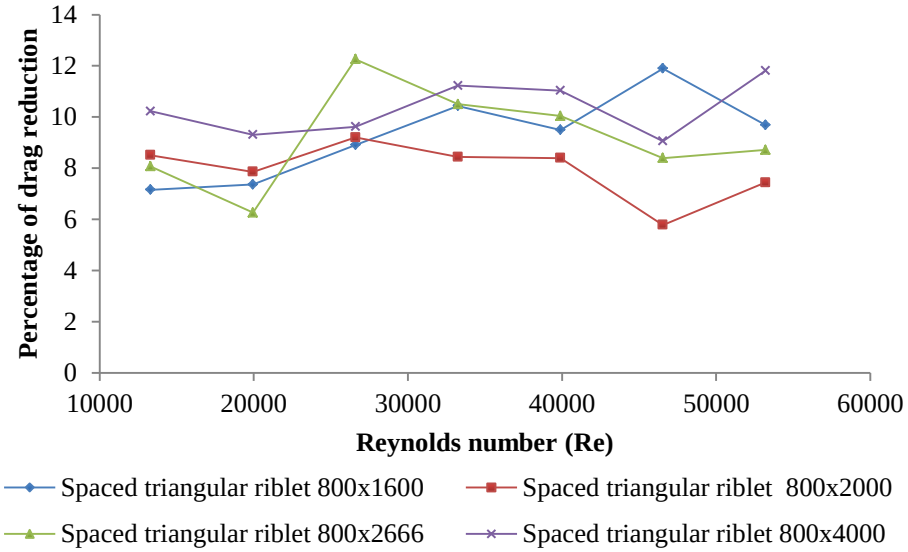

Fig. 14. Effect of Reynolds number on the percentage of drag reduction for spaced triangular riblet.

4. Conclusions

In general, the spaced triangular riblets continue to increase when the Reynolds number increases. Meanwhile, the curve of the spaced triangular riblet with spacing dimensions of $800\ \mu m \times 2666\ \mu m$ initially reaches its maximum at a Reynolds number of 2.6×10^4 with a value of 12.3 and then starts to decline reaching a value of 8.4 at a Reynolds number of 4.6×10^4.

Acknowledgments

This work was supported financially by University Malaysia Pahang (UMP) through the Fundamental Research Grant

References

[1] J. Laufer, "New Trends in Experimental Turbulence Research," *Annual Review of Fluid Mechanics*, vol. 7, pp. 307-326, 1975.
[2] W. Willmarth, "Pressure Fluctuations Beneath Turbulent Boundary Layers," *Annual Review of Fluid Mechanics*, vol. 7, pp. 13-36, 1975.
[3] R. A. Antonia, "Conditional Sampling in Turbulence Measurement," *Annual Review of Fluid Mechanics*, vol. 13, pp. 131-156, 1981.
[4] B. J. Cantwell, "Organized Motion in Turbulent Flow," *Annual Review of Fluid Mechanics*, vol. 13, pp. 457-515, 1981.
[5] H. E. Fiedler, "Coherent Structures," in *Advances in Turbulence*, C. B. Geneviève and M. Jean, Eds., ed Berlin Heidelberg: Springer 1987, pp. 320-336.
[6] R. F. Blackwelder, "Coherent structures associated with turbulent transport," in *Transport Phenomena in Turbulent Flows: Theory, Experiment, and Numerical Simulation*, 1988, pp. 69-88.
[7] S. K. Robinson, "Coherent Motions in the Turbulent Boundary Layer," *Annual Review of Fluid Mechanics*, vol. 23, pp. 601-639, 1991.
[8] S. P. Wilkinson, J. B. Anders, B. S. Lazos, and D. M. Bushnell, "Turbulent drag reduction research at NASA langley: progress and plans," *International Journal of Heat and Fluid Flow*, vol. 9, pp. 266-277, 1988.
[9] M. Gad-el-Hak, "The Art and Science of Flow Control," in *Frontiers in Experimental Fluid Mechanics*. vol. 46, M. Gad-el-Hak, Ed., ed: Springer Berlin Heidelberg, 1989, pp. 211-290.
[10] M. Gad-el-Hak, "Modern Developments In Flow Control," *Applied Mechanics Reviews*, vol. 49, pp. 365-380, 1996.
[11] M. J. Walsh, "Riblets," *Viscous drag reduction in boundary layers*, vol. 1, pp. 203-261, 1990.
[12] A. M. Savill, "Drag Reduction by Passive Devices - a Review of some Recent Developments," in *Structure of Turbulence and Drag Reduction*, ed: Springer Berlin Heidelberg, 1990, pp. 429-465.
[13] F. E. Fish and G. V. Lauder, "Passive and Active Flow Control by Swimming Fishes and Mammals," *Annual Review of Fluid Mechanics*, vol. 38, pp. 193-224, 2006.
[14] A. R. Paul, S. Joshi, A. Jindal, S. P. Maurya, and A. Jain, "Experimental Studies of Active and Passive Flow Control Techniques Applied in a Twin Air-Intake," *The Scientific World Journal*, vol. 2013, p. 8, 2013.
[15] H. A. Abdulbari, H. D. Mahammed, and Z. B. Y. Hassan, "Bio-Inspired Passive Drag Reduction Techniques: A Review," *ChemBioEng Reviews*, vol. 2, pp. 185-203, 2015.
[16] P. Luchini, F. Manzo, and A. Pozzi, "Resistance of a grooved surface to parallel flow and cross-flow," *Journal of Fluid Mechanics*, vol. 228, pp. 87-109, 1991.
[17] S. K. Robinson, "The kinematics of turbulent boundary layer structure," PhD, Stanford University, NASA TM. In press, Stanford, CA, 1991.
[18] J. B. Johansen and C. R. Smith, "The effects of cylindrical surface modifications on turbulent boundary layers," *AIAA Journal*, vol. 24, pp. 1081-1087, 1986/07/01 1986.
[19] D. Hooshmand, R. Youngs, J. Wallace, and J. Balint, "An experimental study of changes in the structure of a turbulent boundary layer due to surface geometry changes," in *21st Aerospace Sciences Meeting*, ed Reno, Nevada: American Institute of Aeronautics and Astronautics, 1983.
[20] K.-S. Choi, "A New Look at the Near-Wall Turbulence Structure," in *Advances in Turbulence*, G. Comte-Bellot and J. Mathieu, Eds., ed: Springer Berlin Heidelberg, 1987, pp. 373-382.
[21] J. Gallagher and A. Thomas, "Turbulent boundary layer characteristics over streamwise grooves," in *2nd Applied Aerodynamics Conference*. vol. 2nd,, ed Seattle, WA: American Institute of Aeronautics and Astronautics, 1984, p. 9.
[22] R. Wahidi, W. Chakroun, and S. Al-Fahed, "The behavior of the skin-friction coefficient of a turbulent boundary layer flow over a flat plate with differently configured transverse square grooves," *Experimental Thermal and Fluid Science*, vol. 30, pp. 141-152, 11// 2005.
[23] J.-j. Wang, S.-l. Lan, and G. Chen, "Experimental study on the turbulent boundary layer flow over riblets surface," *Fluid Dynamics Research*, vol. 27, pp. 217-229, 10// 2000.

[24] B. D and R. W, "On the Drag Reduction of the Shark Skin," in *23rd Aerospace Sciences Meeting*, ed: American Institute of Aeronautics and Astronautics, 1985.
[25] M. J. Walsh, "Riblets as a Viscous Drag Reduction Technique," *AIAA Journal*, vol. 21, pp. 485-486, 1983.
[26] H. Choi, "Turbulent drag reduction: Studies of feedback control and flow over riblets," Ph.D, Mechanical engineering, Stanford University & Thermosciences Division TF-55., Ann Arbor United States, 1993.
[27] E. V. Bacher and C. R. Smith, "Turbulent Boundary-Layer Modification by Surface Riblets," *AIAA Journal*, vol. 24, pp. 1382-1385, 08/01 1986.
[28] R. Grüneberger and W. Hage, "Drag characteristics of longitudinal and transverse riblets at low dimensionless spacings," *Experiments in Fluids*, vol. 50, pp. 363-373, 2011.
[29] K.-S. Choi, "Near-wall structure of a turbulent boundary layer with riblets," *Journal of Fluid Mechanics*, vol. 208, p. 417, 1989.
[30] S. Tardu, T. V. Truong, and B. Tanguay, "Bursting and structure of the turbulence in an internal flow manipulated by riblets," *Applied Scientific Research*, vol. 50, pp. 189-213, 1993.
[31] N. Y. Alkhamis, A. P. Rallabandi, and J.-C. Han, "Heat Transfer and Pressure Drop Correlations for Square Channels With V-Shaped Ribs at High Reynolds Numbers," *Journal of Heat Transfer*, vol. 133, pp. 111901-111901, 2011.
[32] J. M. Wallace, "Experimental Studies of the Structural Changes of the Turbulent Boundary Layer Due to Surface Geometry Changes," in *the Drag Reduction Symposium*, Washington, DC, , 1982.
[33] D. Hooshmand, R. Youngs, and J. M. Wallace, "An experimental study of changes in the structure of a turbulent boundary layer due to surface geometry changes," in *21st Aerospace Sciences Meeting*, ed: American Institute of Aeronautics and Astronautics, 1983.
[34] K.-S. Choi, *Near-wall turbulence structure on a riblet wall*: BMT, 1985.
[35] S.-H. Seo, C.-D. Nam, J.-Y. Han, and C.-H. Hong, "Drag Reduction of a Bluff Body by Grooves Laid Out by Design of Experiment," *Journal of Fluids Engineering*, vol. 135, pp. 111202-111202, 2013.
[36] M. F. Tachie, S. S. Paul, M. Agelinchaab, and M. K. Shah, "Structure of turbulent flow over 90° and 45° transverse ribs," *Journal of Turbulence*, vol. 10, p. N20, 2009/01/01 2009.
[37] M. K. Bull, "WALL-PRESSURE FLUCTUATIONS BENEATH TURBULENT BOUNDARY LAYERS: SOME REFLECTIONS ON FORTY YEARS OF RESEARCH," *Journal of Sound and Vibration*, vol. 190, pp. 299-315, 2/29/ 1996.
[38] A. S. Tijsseling, "FLUID-STRUCTURE INTERACTION IN LIQUID-FILLED PIPE SYSTEMS: A REVIEW," *Journal of Fluids and Structures*, vol. 10, pp. 109-146, 2// 1996.
[39] N. K. Tutu, "Pressure fluctuations and flow pattern recognition in vertical two phase gas-liquid flows," *International Journal of Multiphase Flow*, vol. 8, pp. 443-447, 8// 1982.
[40] M. Qing, Z. Jinghui, L. Yushan, W. Haijun, and D. Quan, "Experimental studies of orifice-induced wall pressure fluctuations and pipe vibration," *International Journal of Pressure Vessels and Piping*, vol. 83, pp. 505-511, 7// 2006.
[41] R. L. Panton, "Review of Wall Turbulence as Described by Composite Expansions," *Applied Mechanics Reviews*, vol. 58, pp. 1-36, 2005.
[42] T. Mullin, "Experimental Studies of Transition to Turbulence in a Pipe," *Annual Review of Fluid Mechanics*, vol. 43, pp. 1-24, 2011.
[43] T. W. Lancey and L. W. Reidy, "Effects of surface riblets on the reduction of wall pressure fluctuations in turbulent boundary layers," *The Journal of the Acoustical Society of America*, vol. 85, pp. 1793-1794, 1989.
[44] W. L. Keith, "Spectral measurements of pressure fluctuations on riblets," *AIAA Journal*, vol. 27, pp. 1822-1824, 1989/12/01 1989.
[45] K.-S. Choi, "The Wall-pressure Fluctuations of Modified Turbulent Boundary Layer with Riblets," in *Turbulence Management and Relaminarisation*, H. W. Liepmann and R. Narasimha, Eds., ed: Springer Berlin Heidelberg, 1988, pp. 149-160.
[46] B. Dean and B. Bhushan, "The effect of riblets in rectangular duct flow," *Applied Surface Science*, vol. 258, pp. 3936-3947, 2/1/ 2012.
[47] G. D. Bixler and B. Bhushan, "Shark skin inspired low-drag microstructured surfaces in closed channel flow," *Journal of Colloid and Interface Science*, vol. 393, pp. 384-396, 3/1/ 2013.
[48] D. W. Green, *Perry's chemical engineers' handbook* vol. 796: McGraw-hill New York, 2008.
[49] S. J. Beresh, J. F. Henfling, R. W. Spillers, and B. O. M. Pruett, "Very-large-scale coherent structures in the wall pressure field beneath a supersonic turbulent boundary layer," *Physics of Fluids*, vol. 25, p. 095104, 2013.
[50] P.-z. Gao, T.-h. Liu, T. Yang, and S.-c. Tan, "Pressure drop fluctuations in periodically fluctuating pipe flow," *Journal of Marine Science and Application*, vol. 9, pp. 317-322, 2010/09/01 2010.
[51] W. W. Willmarth and C. S. Yang, "Wall-pressure fluctuations beneath turbulent boundary layers on a flat plate and a cylinder," *Journal of Fluid Mechanics*, vol. 41, pp. 47-80, 1970.
[52] F. Johnsson, R. C. Zijerveld, J. C. Schouten, C. M. van den Bleek, and B. Leckner, "Characterization of fluidization regimes by time-series analysis of pressure fluctuations," *International Journal of Multiphase Flow*, vol. 26, pp. 663-715, 4/1/ 2000.